

Aqueous Synthesis of Zinc Blende CdTe/CdS Magic-Core/Thick-Shell Tetrahedral-Shaped Nanocrystals with Emission Tunable to Near-Infrared

Zhengtao Deng,^{*,†} Olaf Schulz,[‡] Su Lin,[†] Baoquan Ding,[†] Xiaowei Liu,[†] XiXi Wei,[†] Robert Ros,[‡] Hao Yan,[†] and Yan Liu^{*,†}

The Biodesign Institute, Department of Chemistry and Biochemistry, and Department of Physics, Arizona State University, Tempe, Arizona 85287

Received February 26, 2010; E-mail: yan_liu@asu.edu; zhengtao.deng@asu.edu

Semiconductor nanocrystals (NCs), or quantum dots (QDs), that emit in the near-infrared (NIR) range of 700 to 900 nm are particularly interesting for bioimaging applications because at these wavelengths light has deep tissue penetration and induces minimal autofluorescence.¹ Unfortunately, high-quality NIR NCs have remained elusive, despite pioneering efforts devoted to the preparation of NIR NCs using multistep high-temperature organometallic approaches.² Herein, we report a facile low-temperature aqueous method for synthesizing stable, bright, water-soluble CdTe/CdS magic-core/thick-shell NCs that are tetrahedral-shaped and whose NIR emission can be tuned by varying the shell thickness.

Recently, several groups have demonstrated the synthesis of thick-shell NCs. In 2008, Mahler et al.³ and Chen et al.⁴ reported the synthesis of CdSe/CdS NCs with thick (5 nm) shells that have reduced blinking at the single-NC level. The thick-shell NCs also show significantly more photostability than traditional core/shell NCs. In 2009, Nie and co-workers⁵ described a class of wurtzite CdTe core-based core/shell NCs that are converted into type-II NCs by lattice strain between the soft core and the compressive shell. Very recently, Mahler et al.⁶ synthesized thick-shell CdSe/CdS core/shell NCs in either a pure wurtzite (W) or zinc blende (ZB) structure and observed their reduced blinking behavior. These findings indicate that thick-shell NCs might be an effective strategy toward developing NCs that exhibit less blinking and greater photostability and thus may represent a new route for achieving next-generation NCs.

Previous thick-shell NCs were obtained by multistep high-temperature organometallic approaches.^{3–6} Moreover, because of the large core size, the reported thick-shell structure inevitably led to large NCs (>13 nm), which are disadvantageous for intracellular imaging.⁷ Herein, we report the synthesis of thick-shell NCs directly in aqueous solution and the first use of a magic-sized CdTe core to achieve thick-shell NCs with NIR emission. This new synthesis method allows better tunability of the photoluminescence (PL) emission (480–820 nm) and maintains relatively small sizes of the resulting thick-shell NCs, e.g., a hydrodynamic diameter of ~11.0 nm for NCs with an emission maximum at 820 nm.

Our strategy was modeled on the classic aqueous methods for synthesis of NCs, which involve refluxing of a metal–thiol complex with NaHTe or NaHSe precursors.⁸ Briefly, magic-sized CdTe clusters with a radius of ~0.8 nm were first synthesized, as verified by the UV–vis absorption (peak at 465 nm) and band-edge emission (maximum at 480 nm) spectra (Figure S1A in the Supporting Information). Furthermore, these magic-sized clusters were identified by time-of-flight (TOF) mass spectrometry (MS) and high-resolution transmission electron microscopy (HRTEM) (Figure S1B,C). Next, a thick CdS shell was grown over the magic-sized clusters by decomposing the Cd–thiol complex, affording CdTe/CdS magic-core/thick-shell NCs with shell thicknesses of up to 5 nm. Experimental details and characterizations are described in the Supporting Information (Figures S1–S5).

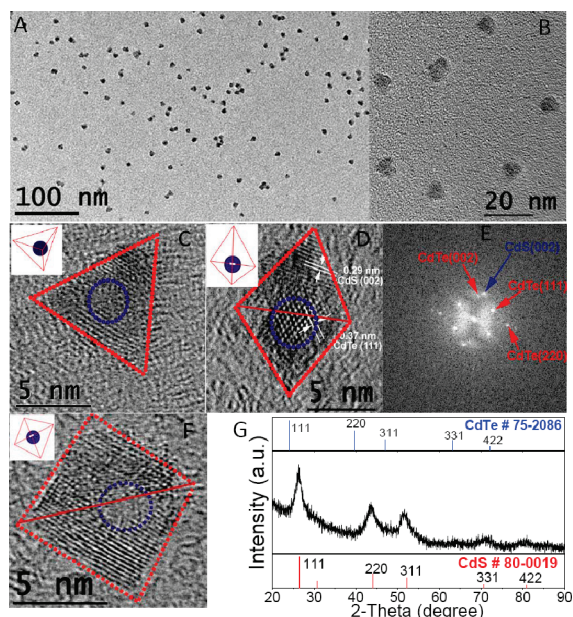


Figure 1. (A, B) TEM images of the CdTe/CdS magic-core/thick-shell tetrahedral-shaped NCs with an emission maximum at 820 nm. (C, D, F) High-magnification TEM images of three typical tetrahedral NCs with different projections. The insets show schematic drawings of the NCs; blue circles illustrate the CdTe cores, while the red lines mark the geometries of the tetrahedral NCs. (E) Indexed FFTs of a single tetrahedral NC shown in (D). (G) XRD pattern and reference patterns (blue and red vertical lines) from the JCPDS cards.

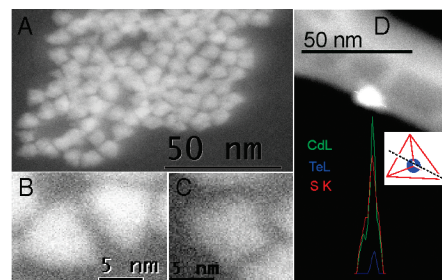


Figure 2. (A–C) HAADF-STEM images of tetrahedral NCs with an emission maximum at 820 nm. (D) STEM-EDS line scan along a single tetrahedral NC. The green, blue, and red patterns show the distribution of each element along the white line across the NC. The inset shows the corresponding schematic drawing.

TEM (Figure 1A,B and Figure S6) and high-angle annular dark-field scanning transmission electron microscopy (HAADF-STEM) images (Figure 2A and Figures S7 and S8) demonstrate that the typical thick-shell NCs with an emission maximum at 820 nm were nearly monodispersed. Detailed HRTEM and STEM images show that these NCs have tetrahedral morphology, with each edge having a length of

[†] The Biodesign Institute, Department of Chemistry and Biochemistry.

[‡] Department of Physics.

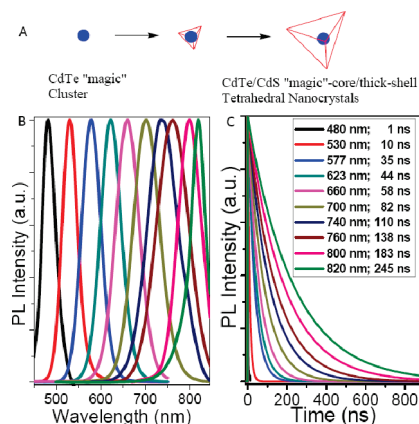


Figure 3. (A) Schematic diagram illustrating the formation of the CdTe/CdS magic-core/thick-shell tetrahedral NCs. (B) Room-temperature PL emission profiles of a series of NC samples obtained by varying the CdS shell growth to overcoat the magic-sized CdTe core with thicker shells. (C) Room-temperature PL decay kinetics monitored at the maximum emission wavelengths of the samples in (B). The calculated excited state lifetimes are listed.

~10 nm (Figures 1C,D,F and 2B,C and Figures S6 and S7). Because of the large lattice mismatch (10%) between the CdTe core and the CdS shell, we can unambiguously determine the core-shell boundary of the thick-shell NCs from the HRTEM images (Figure 1C,D,F); this has not been achieved previously for CdSe/CdS or CdTe/ZnSe thick-shell NCs.^{3–6} The well-resolved lattice images and the indexed fast Fourier transforms (FFTs) (Figure 1E) indicate a well-resolved CdTe/CdS core/shell structure. Moreover, as shown in Figure 2D and Figure S8, STEM-energy-dispersive X-ray spectroscopy (EDS) line scans through the center of a single thick-shell NCs reveal the presence of Cd and S spanning the entire width of the particle while Te is confined to the narrow domain of the core, indicating an obvious core/shell structure.⁹ The X-ray diffraction (XRD) pattern of the sample (Figure 1G) can be indexed to a cubic ZB phase; the diffraction peaks are close to the pure CdS phase but slightly shifted to smaller angles. These results all indicate the formation of high-quality CdTe/CdS magic-core/thick-shell tetrahedral-shaped NCs. It is noted that Mahler et al.⁶ also observed the formation of tetrahedral-shaped ZB CdSe/CdS thick-shell NCs by the high-temperature organometallic approach.

A schematic diagram of the formation of the CdTe/CdS magic-core/thick-shell tetrahedral NCs is shown in Figure 3A. The PL emission wavelength can be continuously tuned across the visible spectrum to the NIR region (Figure 3B) by adjusting the thickness of the CdS shell, which can be easily controlled by varying the reaction temperature and reaction time (Figures S1–S4). The magic-sized CdTe core has a PL peak at 480 nm, and a series of core/shell NCs with band-edge emission maxima at 530, 577, 623, 660, 700, 740, 760, 800, and 820 nm were obtained, with typical PL quantum yields up to 70% (Figure S5). These thick-shell NCs prepared in aqueous solution also have better photostability than those produced using the ligand-exchange method (Figure S9B). In addition, these NCs have compact sizes, e.g., the hydrodynamic diameters obtained using dynamic light scattering (DLS) were ~6.7, ~9.3, and ~11.0 nm for NCs with emission maxima at 700, 760, and 820 nm, respectively (Figures S9–S11).

Figure 3C shows their corresponding emission decay curves, which reveal a dramatic increase in the NC emission lifetime by 2 orders of magnitude (from 1 to 245 ns) after overcoating CdTe core with the thick CdS shell. The enormous red shift (~340 nm) of the PL emission peaks and significant increase (~245-fold) in the lifetime indicates a transition from type-I to type-II NCs during the well-controlled gradual growth of the shell. This is possibly due to band-edge shifts of the core and shell induced by the opposite lattice strains they experience, as suggested by Nie and co-workers.⁵

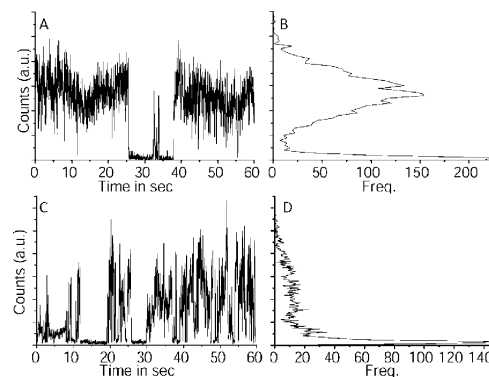


Figure 4. Typical fluorescence intensity time traces for single CdTe/CdS NCs with shell thickness of (A) ~3 nm and (C) ~1 nm. (B, D) Intensity distributions corresponding to (A) and (C).

To evaluate their blinking behavior, well-dispersed thick-shell and thin-shell NCs were imaged with a confocal fluorescence microscope (MicroTime 200, PicoQuant, Germany). Figure 4A,B and Figure S12 show time traces of the fluorescence intensity for the CdTe/CdS NCs with shell thicknesses of ~3 and ~1 nm, respectively, indicating blinking reduction for the thick-shell NCs. The larger number of long on-times for the thick-shell NCs (Figure S13) suggests significantly suppressed blinking behavior for all of the measured thick-shell NCs in comparison with the thin-shell NCs.

In conclusion, we have developed a simple aqueous method for the synthesis of stable and bright NIR-emitting water-soluble CdTe/CdS magic-core/thick-shell tetrahedral-shaped nanocrystals. Strong shell-thickness dependence of the PL emission wavelength and PL lifetime were observed. We believe these thick-shell NCs could find broad use in multicolor bioimaging, biosensing, solar cells, and other nanodevice applications.

Acknowledgment. We thank Dr. Z. Liu, Dr. E. Soignard, Dr. R. Varghese, and Dr. Y. Tian for technical assistance with HRTEM, XRD, MS, and DLS. We are grateful for funding support from ONR, ARO, NSF, and NIH to Y.L., support from ONR, NSF, NIH, ARO, AFOSR, and DOE and a Sloan Research Fellowship to H.Y., and support from ASU to R.R.; Y.L. and H.Y. were supported as part of the Center for Bio-Inspired Solar Fuel Production, an Energy Frontier Research Center funded by the U.S. Department of Energy, Office of Science, Office of Basic Energy Sciences, under Award DE-SC0001016.

Supporting Information Available: Additional synthesis and characterization details and Figures S1–S13. This material is available free of charge via the Internet at <http://pubs.acs.org>.

References

- (1) Kim, S.; Lim, Y. T.; Soltesz, E. G.; De Grand, A. M.; Lee, J.; Nakayama, A.; Parker, J. A.; Mihaljevic, T.; Laurence, R. G.; Dor, D. M.; Cohn, L. H.; Bawendi, M. G.; Frangioni, J. V. *Nat. Biotechnol.* **2004**, *22*, 93. Hinds, S.; Myrskog, S.; Levina, L.; Koleilat, G.; Yang, J.; Kelley, S. O.; Sargent, E. H. *J. Am. Chem. Soc.* **2007**, *129*, 7218.
- (2) Choi, H. S.; Ipe, B. I.; Misra, P.; Lee, J. H.; Bawendi, M. G.; Frangioni, J. V. *Nano Lett.* **2009**, *9*, 2354. Xie, R.; Chen, K.; Chen, X.; Peng, X. *Nano Res.* **2008**, *1*, 457.
- (3) Mahler, B.; Spinicelli, P.; Buil, S.; Quelin, X.; Hermier, J.-P.; Dubertret, B. *Nat. Mater.* **2008**, *7*, 659.
- (4) Chen, Y.; Vela, J.; Htoon, H.; Casson, J. L.; Werder, D. J.; Bussian, D. A.; Klimov, V. I.; Hollingsworth, J. A. *J. Am. Chem. Soc.* **2008**, *130*, 5026.
- (5) Smith, A. M.; Mohs, A. M.; Nie, S. *Nat. Nanotechnol.* **2009**, *4*, 56.
- (6) Mahler, B.; Lequeux, N.; Dubertret, B. *J. Am. Chem. Soc.* **2010**, *132*, 953.
- (7) Smith, A. M.; Nie, S. *Nat. Biotechnol.* **2009**, *27*, 732.
- (8) Rogach, A. L.; Katsikas, L.; Kornowski, A.; Su, D.; Eychmüller, A.; Weller, H. *Ber. Bunsen-Ges. Phys. Chem.* **1996**, *100*, 1772. He, Y.; Lu, H.; Sai, L.; Su, Y.; Hu, M.; Fan, C.; Huang, W.; Wang, L. *Adv. Mater.* **2008**, *20*, 3416. Zou, L.; Gu, Z.; Zhang, N.; Zhang, Y.; Fang, Z.; Zhu, W.; Zhong, X. *J. Mater. Chem.* **2008**, *18*, 2807. Deng, Z. T.; Lie, F. L.; Shen, S. Y.; Ghosh, I.; Mansuripur, M.; Muscat, A. J. *Langmuir* **2009**, *25*, 434.
- (9) Deng, Z. T.; Yan, H.; Liu, Y. *J. Am. Chem. Soc.* **2009**, *131*, 17744.

JA101476B